NARROWBAND SOURCE LOCALISATION IN THE DEEP OCEAN USING A NEAR-SURFACE ARRAY

Rui Duan[1], Kunde Yang[1] and Yuanliang Ma[1]

[1]Institute of Acoustic Engineering, Northwestern Polytechnical University, Xi'an 710072, China

Corresponding author: Kunde Yang E-mail: ykdzym@nwpu.edu.cn

A narrowband source at moderate range can be localised in a deep ocean using a near-surface vertical linear array without knowing the bottom properties. By casting the localisation as separate estimations of the source range and source depth, the performance is much better than that of the matched-field-processing (MFP) technique with the Bartlett processor. Source range estimation is based on the weighted subspace fitting technique with modification to consider the array tilt. Source depth estimation is based on the time delay of multipath arrivals. Experimental results using explosive sources are shown. The presented method shows a significant improvement in performance.

PACS: 43.30.Cq, 43.30.Wi

INTRODUCTION

The MFP technique for narrowband source localisation has been analysed widely [1], [2]. It has been pointed out that its performance is poor when the array aperture is limited or the ocean environment is uncertain [3], especially when the bottom properties are unknown. In contrast, the arrival structures of the multiple arrivals that do not penetrate into buried layers, are much more stable. Furthermore, in the deep ocean the information of source range and source depth is included primarily in arrival angles and time delays [4], respectively. Therefore, the localisation can be casted as separate estimations of the source range and source depth.

The "weighted-subspace-fitting matched field (WSF-MF) technique" for passive narrowband source localisation developed by Duan *et al*. [5], is to minimise the distance between the signal subspace and the space spanned by the array manifold in a finite range-depth space. The information of arrival angles is contained in the signal subspace and thus this technique does not estimate the arrival angles. However, as only the arrival angles are used, the method is only effective in the estimation of source range. The array tilt [6] caused by the ocean current would reduce the performance of the WSF-MF technique. Therefore, a modified approach of the WSF-MF technique considering the array tilt is used to estimate the source range. Then, a method based on the time delays between multipath arrivals is presented to determine the source depth. By combining the above two methods, the source location can be estimated more accurately.

The data with explosive sources collected during an experiment in the deep ocean is used to verify the modified WSF-MF technique and the depth-estimation method. The detailed description of the experiment and the results are shown in Section 3 and Section 4, respectively.

LOCALISATION APPROACH

Modified WSF-MF method

An overview of the detailed WSF-MF technique [5] is as follows. In the deep ocean, it is assumed that the array aperture is rather small and the source is in the far field. Therefore, the K multipath arrivals can be modeled as K plane waves. Consider a uniform linear array (ULA) of M elements. It is assumed that K narrowband arrivals impinge on it from directions Θ_0 being $[\Theta_1, \Theta_2, \dots, \Theta_k, \dots, \Theta_K]^T$, where Θ_k is the arrival angle of the kth arrival. Then, the M-vector of hydrophone outputs are

$$\mathrm{y}(t) = \mathrm{A}(\Theta_0)\mathrm{s}(t)+\mathrm{n}(t), \tag{1}$$

where the array manifold $\mathrm{A}(\Theta_0)$ is a $M \times K$ matrix whose kth column $\mathrm{a}(\Theta_k)$ is the steering vector for the kth arrival, $\mathrm{s}(t)$ is the $K\times 1$ signal vector, and $\mathrm{n}(t)$ is the $M\times 1$ noise vector and the noise at different hydrophones is uncorrelated. It is assumed that the signals and noise are complex-valued and are statistically independent of each other. The noise is a stationary, zero-mean, Gaussian process. It is noted that the matrix $\mathrm{A}(\Theta_0)$ can be simplified for a ULA [7]. The eigen-decomposition of the array covariance is expressed as

$$\mathrm{R_y}=\mathrm{E}(\mathrm{y}(t)\mathrm{y}^H(t)) = \mathrm{U}_s\Lambda_s\mathrm{U}_s^H + \sigma^2\mathrm{U}_n\mathrm{U}_n^H, \tag{2}$$

where, Λ_s contains the K' largest eigenvalues. K' is the rank of the signal covariance. The signal subspace U_s is the set of corresponding eigenvectors, σ^2 is the variance of the noise, and the noise subspace U_n contains the M-K' eigenvectors. By minimising the distance between the signal subspace and the space spanned by the array manifold [8], the arrival angles Θ_0 are given by

$$\tilde{\Theta}_0 = \min\|\mathrm{U}_s\mathrm{V}^{1/2} - \mathrm{A}(\Theta)\mathrm{B}\|_F^2, \tag{3}$$

where $\|.\|_F$ denotes the Frobenius norm, V is a positive definite weighting matrix. To give the lowest asymptotic variance [8], V equals $\Lambda^2\Lambda_s^{-1}$, where Λ is $\Lambda_s - \sigma^2\mathrm{I}$. Solving Eq. (3) for B and substituting back into Eq. (3), one obtains

$$\tilde{\Theta}_0 = \min\, tr\{P_{\mathrm{A}}^{\perp}(\Theta)\mathrm{U}_s\mathrm{V}\mathrm{U}_s^H\}, \tag{4}$$

where A is the array manifold in Eq. (3), $P_A^{\perp}(\Theta)$= I-P_A=I-AA^{+}=I-$A(A^H A)^{-1}A^H$ and $tr\{.\}$ denotes the trace of a matrix.

The hypothesised source location is denoted by $L_h=[z,r]$, where z is the source depth from the ocean surface and r is the horizontal range from the array. The arrival angles of the multipath arrivals on the array are the function of the hypothesised source location. This function can be expressed as

$$\Theta_h = g(L_h), \tag{5}$$

where g (.) is determined by the acoustic environment and can be calculated using the standard ray approach. Substituting Eq. (5) into Eq. (4), one obtains

$$\tilde{L}_o = \min tr\{P_A^{\perp}(g(L_h))U_s V U_s^H\}, \tag{6}$$

where the parameters U_s and V are calculated from the received signal, and the value of $P_A^{\perp}$ ($g(L_h)$) is only determined by the hypothesised source location L_h. Therefore, the estimated source location $\tilde{L}_o$ can be given by searching the finite range-depth space of L_h to satisfy Eq. (6).

Considering the array tilt in the ocean environment, the real arrival angles may deviate from the ideal arrival angles by a random variable φ, which increase the distance between the signal subspace and the space spanned by the array manifold at the real source location. Therefore, for a certain hypothesised source location the corresponding array manifold should take the random variable φ into consideration. It can be accomplished by searching the interval of φ to get the minimum distance. That is

$$\tilde{L}_o = \min_{L_h}\{ \min_{\varphi\in[\varphi_{\min},\varphi_{\max}]} tr\{P_{A(\Theta_h+\varphi)}^{\perp}(g(L_h))U_s V U_s^H\}\}, \tag{7}$$

where $\varphi_{\min}$ and $\varphi_{\max}$ are the lower and upper bounds of the array tilt angle.

The ambiguity surface of the source locations corresponding to the modified WSF-MF method is defined as

$$E_W = \frac{1}{tr\{P_{A(\Theta_h+\varphi)}^{\perp}(g(L_h))U_s V U_s^H\}}\ . \tag{8}$$

It is noted that E_W is a cost function of three unknown parameters, r, z and φ. The normalised ambiguity surface in dB is defined as

$$E_N = 10\log_{10}\left(\frac{E_W}{\max(E_W)}\right). \tag{9}$$

It is noted that searching the interval of φ might give rise to false peaks in the ambiguity surface. For example, if the arrival angles corresponding to the real source location are Θ_0, the sum $\Theta_0 + \varphi$ may correspond to arrival angles at another source-depth grid. However, when the vertical linear array is near the ocean surface the introduction of the variable φ cannot give rise to the false peaks. It stems from the fact that the multipath arrivals are in pairs. In a pair, the first arrival is last reflected by the bottom while the second arrival is last reflected by the surface. The propagation path of an arrival is close to the path corresponding to its counterpart. For example, the bottom-reflected (B) and the bottom-surface-reflected (BS) arrivals are a pair of arrivals. The arrival angles of this pair of arrivals are almost symmetric about the horizontal direction as shown in Figure 1(a) and Figure 1(b), where the arrival angles of the B and the BS arrivals on a hydrophone of 60 m in depth are presented, respectively. Therefore, the arrival angles of multipath arrivals are almost symmetric under a near-surface vertical linear array. If Θ_0 is symmetric, $\Theta_0 + \varphi$ is not. That is, no source-depth grid would correspond to the arrival angles $\Theta_0 + \varphi$ and thus no false peaks would appear. The modified WSF-MF method is feasible when the vertical array is near the ocean surface.

It should be mentioned that the method is applicable whether the surface duct exists or not. The arrival angles of the bottom-reflected arrivals are little affected by the surface duct when these arrivals are in the surface duct and are not close to being cut off by that duct. Besides, the arrival angle of the surface duct arrival is around zero and it contributes little to the localisation of the source.

Depth estimation method

It has been demonstrated in [5] that the WSF-MF is effective in the estimation of the source range but not the source depth. Figure 1(a) and Figure 1(b) show that the arrival angles of the B and the BS arrivals are much more sensitive to the range change than to the depth change. As a result, the localisation results would be ambiguous along the depth direction. The information of source depth is included in the time delay between the multipath arrivals, especially for that between the B and the surface-bottom-reflected (SB) arrivals when the source is at the moderate range. It should be mentioned that the moderate range refers to the range where these arrivals are not close to be cut off by the SSP (Sound-Speed Profile). Hereafter, angles measured downward (from the hydrophone) are positive. Figure 1(a) shows that the arrival angles of the B arrival are smaller than 5º when the range is beyond 28 km and this arrival is close to be cut off. Therefore, the moderate range in this environment refers to the range smaller than 28 km. Figure 1(c) shows the time delays between the B and the SB arrivals. The time delay is more sensitive to the depth change than to the range change especially for a shallow source. Therefore, the source depth can be determined by comparing the simulated and the measured time delays as in the following steps:

First, using the standard ray approach with the source range estimated by the modified WSF-MF method, the arrival angles of the B and SB arrivals can be calculated. For a shallow source and shallow hydrophones, the two arrival angles are very close to each other. Second, a spatial filter is designed to get the signal consisting of the B and SB arrivals. Third, the autocorrelation function of the signal is calculated and the time delay between the two arrivals, which is denoted by T_m, is given by the strongest peak except for the peak at the origin. Fourth, the estimated time delay is subtracted by the time

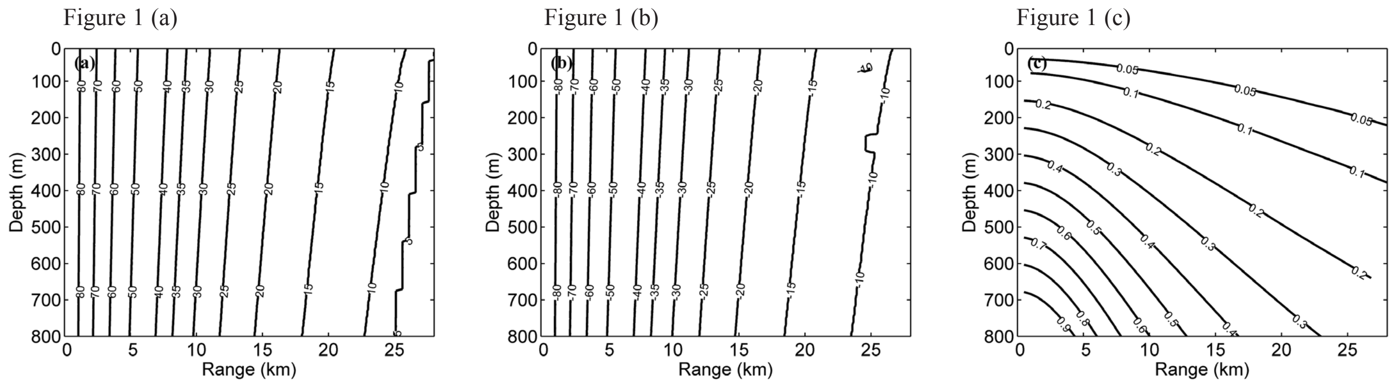

Figure 1 Simulated arrival angles and time delays on a hydrophone at a depth of 60 m under different source locations. The ocean depth is 3500 m. (a) Arrival angles of B arrival. (b) Arrival angles of BS arrival. (c) Time delays between the B and the SB arrivals.

delays at every range-depth grids calculated by the standard ray approach. Finally, the candidates for source location are at the grids with minimum difference. This method is referred to as the time delay of arrivals (TDOA) localisation method. The ambiguity surface is defined as

$$E_T = -|T_m - T(L_h)|, \tag{10}$$

where T_m is the time delay between the B and SB arrivals, and is extracted from the received signals. $T(L_h)$ is the time delay between the two arrivals at the hypothesised source location L_h and is calculated by the standard ray approach. E_T is the time difference between these two parameters. When the hypothesised source location is the same with the real source location, E_T is maximum and is 0 s.

It is noted that the ambiguity surface based on the TDOA method would be ambiguous along the contour of the time delays where the measured time delay stays constant. As the variation with depth is weak, the source depth can be estimated by combining the TDOA method with the source range estimated by the modified WSF-MF method. The ambiguity surface of the combined method is given by

$$E_C = \frac{E_N}{|m(E_N)|} + \frac{E_T}{|m(E_T)|}, \tag{11}$$

where E_N and E_T are the ambiguity surfaces of the modified WSF-MF method and the TDOA method, respectively. $|m(E_N)|$ and $|m(E_T)|$ are the absolute values of the averages of the E_N and E_T, respectively. Eq. (11) is an ad hoc cost function and E_C is dimensionless.

DESCRIPTION OF THE EXPERIMENT

Experimental geometry and the ship track

The experiment was performed in the South China Sea. In the experimental area, the ocean bottom is almost flat and the ocean depth is 3450 m. A vertical Uniform Linear Array of 18 hydrophones spaced at 3.8 m was deployed near the ocean surface. The topmost hydrophone was 20 m below the ocean surface. The vertical array was moving slowly due to the ocean surface wave and subsurface ocean current during the experiment. A GPS receiver was on the buoy float to track the location of the vertical array. The explosive sources were deployed when the ship was moving away from the vertical array to a distance of 40 km. The preset explosive depth was 300 m and the mass of TNT in the explosive charges was 1 kg. The first bubble pulse period calculated by the method in Chapman [9] is 0.0177s. During the experiment, narrowband signals transmitted from a fixed source were also recorded. The source-array range was fixed to be about 8 km (the source level is not high enough for farther measurement). Therefore, the explosions were used to cover different ranges.

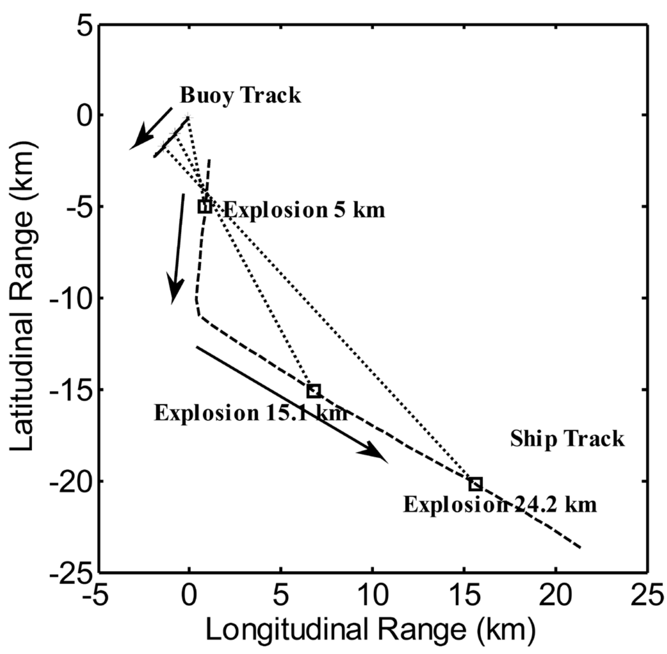

Figure 2 Illustration of the experiment. The motions of the buoy and the ship are shown by the solid line and dashed line, respectively. The geometries of three explosions relative to the buoy are denoted by the dotted lines.

The buoy and the ship tracks together with the direction of motion are shown in Figure 2. The buoy floated southwest and was driven by the prevailing wind. The ship moved south at first and then turned to southeast. The geometries of three explosions relative to the buoy are denoted by the dotted lines. The distances between the array and the three explosions are 5 km, 15.1 km and 24.2 km, respectively. Given that the currents were small and had little shear, the array tilt in such an environment would usually be opposite to the direction of motion of the buoy. It would result in the shifts of the arrival angles of the multipath arrivals impinging on the array. The array tilt is related with the motion speed of the buoy, the mechanical structure of the buoy, the currents etc. The model to calculate the tilt is complicated and is out of the scope of this paper.

Water column sound speed profile

The Conductivity-Temperature-Depth (CTD) sensor was used to measure the SSP before the experiment. The smoothed SSP is shown in Figure 3. It is observed that the surface duct with thickness 40 m exists and the average of the sound speeds in the surface duct is 1539 m/s.

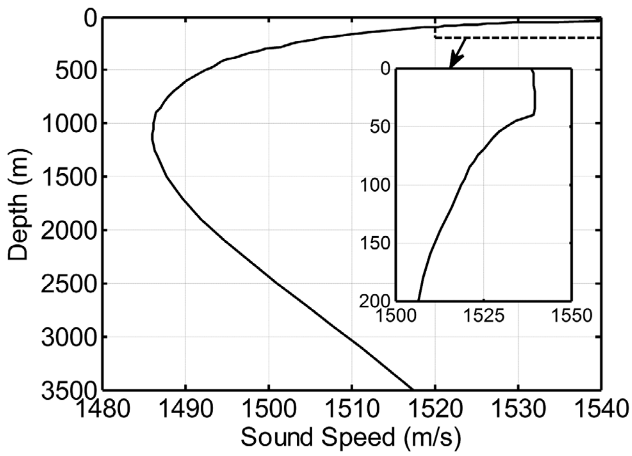

Figure 3 Sound-speed profile at the experiment location. The sound speeds above 1500 m were measured by the CTD before the experiment and the sound speeds below 1500 m were historical data (Simple Ocean Data Assimilation dataset).

Received signals

As the explosions and the array were both shallow, the received signals at moderate range (5 – 28 km) were dominated by the arrivals interacting with the ocean bottom. An example of the received signals of 18 channels is shown in Figure 4(a), where the source range is about 15.1 km. The surface duct arrival and the two groups of multipath arrivals are observed. Here, a group of arrivals denotes the arrivals having the same number of bottom reflections, which are one for the first group and two for the second group in Figure 4(a). As the source level of the explosive source was high, the signal-to-noise ratio (SNR) of the received signals was also high. Figure 4(b) shows the first group of arrivals in detail. From left to the right, the red lines denote the B, BS, SB and SBS arrivals generated by the shock pulse, respectively, and the yellow lines are the corresponding arrivals generated by the first bubble pulse. The time delay between the shock pulse and the first bubble pulse is about 0.017s from Figure 4(b). It is very close to the value calculated by the method in Chapman [9]. It is noted that the arrival times of the surface duct arrival, the first group and the second group are 9.86s, 11.03s and 13.56s, respectively, which are very close to the ray-tracing results, 9.84s, 11.00s and 13.57s correspondingly.

Figure 4 (a)

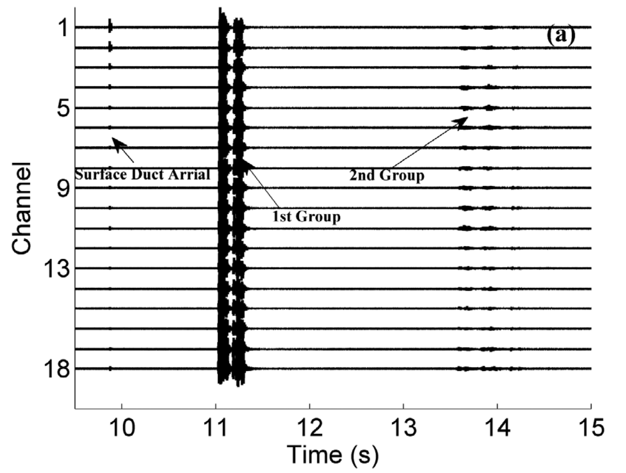

Figure 4 (b)

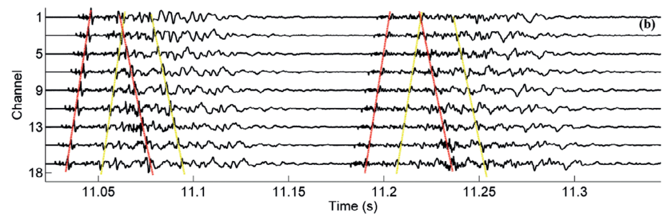

Figure 4 Received signals when the explosion is at 15.1 km. (a) Multipath arrivals impinging on all the hydrophones. The time axis begins at the instant of detonation. (b) Four obvious arrivals in the first group.

Signal preprocessing

This paper is aimed to verify the localisation methods for the narrowband signal under low SNR. Therefore, preprocessing of the signal was performed to obtain the desired signal. It is very important to demonstrate the frequency band within which the method is applicable using the array. Since the optimum wavelength for the array is 7.6 m, the optimum frequency for the array with the sound-speed of 1539 m/s would be 202.5 Hz. Provided that the signal frequency is below 202.5 Hz, the array would sample the depth-dependence of the acoustic field properly and consequently there would be no aliasing in plots of acoustic energy versus direction-of-arrival (DOA). However, when the ocean environment is taken into consideration the frequency band could be wider. It is shown in Figures 1(a) and (b) that when the source range is farther than 5 km, the DOA interval of the multipath arrivals in the first group is about from -50º to 50º. It indicates that when we focus on the sources at the moderate range, most of the signal energy would be limited in this DOA interval. Therefore, with it as *a*

Figure 5 (a)

Figure 5 (b)

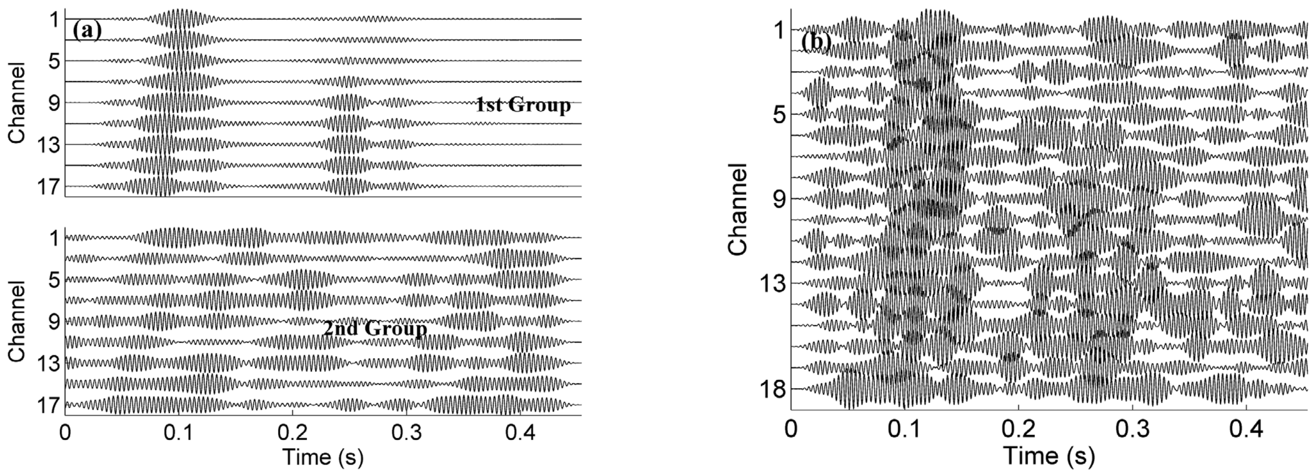

Figure 5 Illustration of the preprocessing of signals. (a) Time alignment of the two groups of multipath arrivals. (b) Narrowband signals with additive narrowband noise.

priori the proper frequency can refer to the one that does not bring in aliasing in this smaller DOA interval, rather than the interval from -90º to 90º. For a ULA, the wavelength should satisfy [10]

$$\frac{\lambda}{d} < 2\sin\Theta, \tag{12}$$

where λ is the wavelength, d is the spacing between the hydrophones and Θ is the maximum arrival angle. Consequently, the maximum frequency is 264 Hz based on this criterion.

Although the WSF has a high angular resolution, the performance may deteriorate with the decreasing SNR and the increasing position errors of the hydrophones. Therefore, the lower bound of the frequency band is estimated roughly using the Rayleigh resolution limit [10], which is

$$\alpha = \arcsin(\lambda/ (Nd)), \tag{13}$$

where N is the number of the hydrophones. If the source range is within 28 km, the minimum DOA difference between the B and the BS arrivals from Figure 1 is about 10º and consequently the maximum wavelength from Eq. (13) is 12 m. Therefore, the lower bound of the frequency band is about 130 Hz. In conclusion, with the frequency within 130 Hz to 264 Hz, the method is applicable for the source localisation when the source is at the moderate range (5 km to 28 km). The frequency band must be reduced when the possible range interval of source becomes larger (e.g. 3 km to 30 km).

In the following, the narrowband signal with centre frequency 260 Hz would be analysed. Firstly, the obvious groups of multipath arrivals were extracted separately and processed by a narrowband filter. Then all groups were aligned with the first group to the start time of the time window for extracting the first group as shown in Figure 5(a), where the two groups of odd channels shown in Figure 4(a) are aligned in time. To retain the phase difference between groups, every group was multiplied by a corresponding phase term which was expressed as

$$p_i = e^{-j2\pi f(t_i - t_1)}, \tag{14}$$

where t_i is the start time of the time window for extracting the ith group and f is the centre frequency of the filter. Secondly, the ocean noise recorded between two explosive sources was filtered using the same filter as that in the first step. Then, the noise was amplified according to the desired SNR. Finally, the desired signal was obtained by adding the amplified noise to the narrowband signal. Figure 5(b) shows the desired signals under SNR 0 dB, where the centre frequency of the filter is 260 Hz and the bandwidth of the filter is 26 Hz.

RESULTS AND DISCUSSION

Modified WSF-MF method

For a SNR of 0 dB, the ambiguity surfaces using Eq.(9) are shown in Figure 6(a), where from the top to bottom panels the source ranges are 5 km, 15.1 km and 24.2 km, respectively. The lower and upper bounds of array tilt angle, φ_{min} and φ_{max} in Eq.(8), are chosen to be -10º and 10º, respectively. The centre frequency of the filter was 260 Hz. The real source locations are denoted by the asterisks.

The ambiguity surfaces present sloping straight striations across the real source locations. As it is shown in Figures 1(a) and 1(b), the contours of the arrival angles in the deep ocean are almost vertical and thus the modified WSF-MF can give a rough estimation of the source range using only the information of the arrival angles. However, this method fails in estimating the source depth. Along the depth direction the spaces spanned by the array manifold in Eq.(3) are very similar. Therefore, the signal space must be estimated accurately and agrees pretty well with the space spanned by the array manifold when the hypothesised source location is the same with the real source location. However, due to the low SNR and signal phase

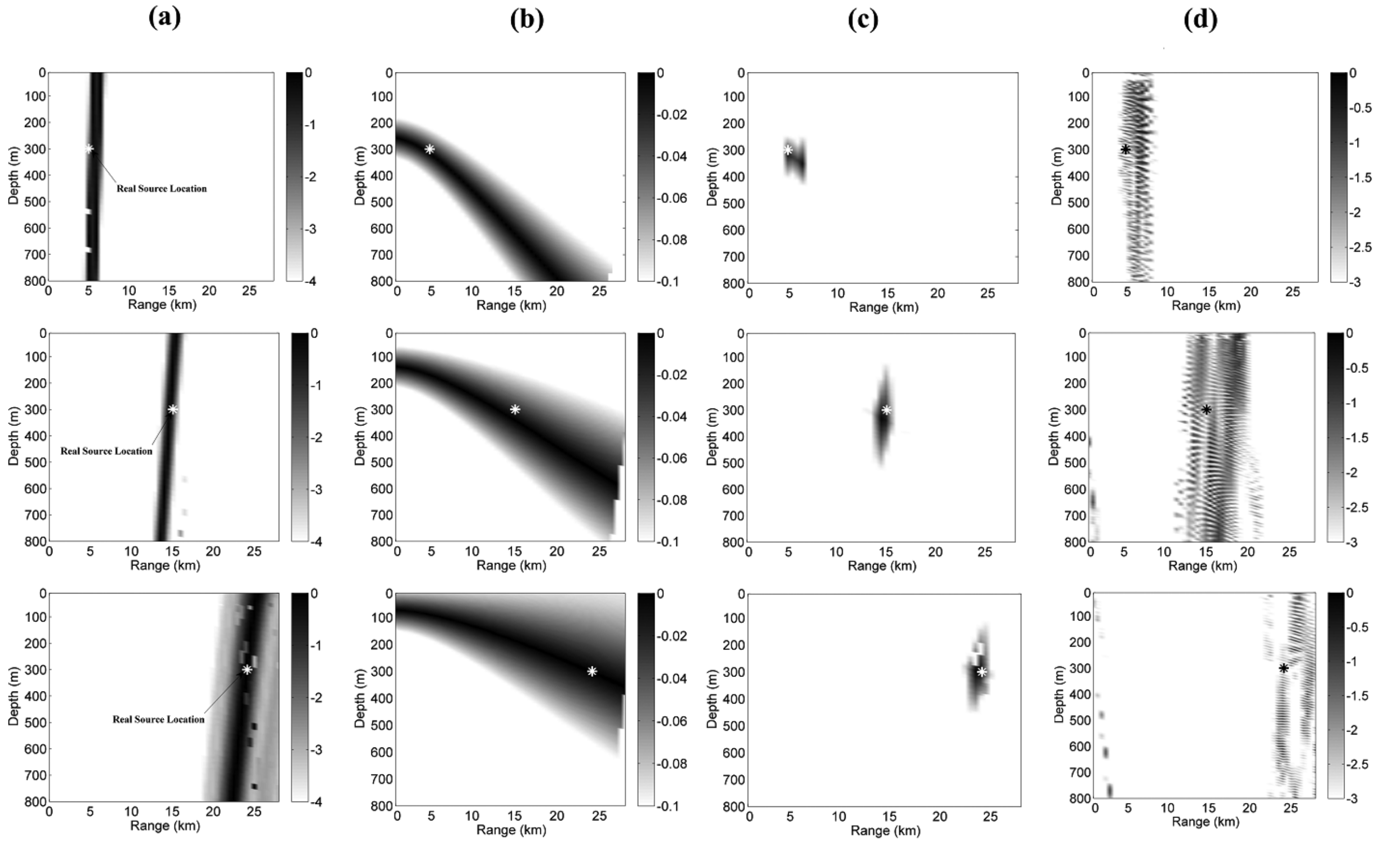

Figure 6 Source localisation results using four methods. From top to bottom panels, the source ranges are 5 km, 15.1 km and 24.2 km, respectively. The source depths are 300 m. The real source locations are denoted by the asterisks. (a) Modified WSF-MF method. (b) TDOA method. (c) Modified WSF-MF method combined with the TDOA method. (d) MFP technique using the Bartlett processor.

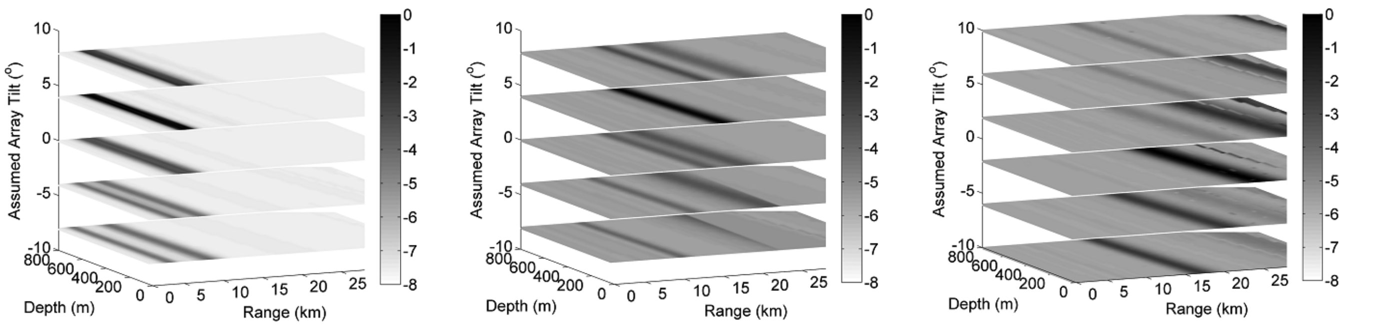

Figure 7 Ambiguity surfaces of the modified WSF-MF method under different array tilt angles. From the left to the right panels, the source ranges are 5 km, 15.1 km and 24.2 km, respectively.

fluctuation, the signal space is inaccurate, which results in the ambiguity along the depth direction.

Eq.(8) introduces the array tilt angle φ as an unknown parameter. The inversion of this parameter can be achieved by drawing pseudo-color plots over the R-Z plane for various values of φ (fixed for each plot), and selecting the plot that yields the smallest overall cost. Figure 7 shows the plots of Eq.(9) over the R-Z plane for some values of φ. From the left to the right panels, the source ranges are 5 km, 15.1 km and 24.2 km respectively. In the first two panels, when the assumed array tilt is 4° the plot yields the strongest overall value. Therefore, the array tilt angles are both 4° when the source ranges are 5 km and 15.1 km. In contrast, the array tilts towards another direction (-2º) when the source range is 24.2 km.

TDOA method

The first step of the TDOA method (see Section 2.2) is the estimation of the arrival angles of the B and SB arrivals based on the WSF-MF method's result. The arrival angle of either of the two arrivals presents little change when the source is along the dark striations in Figure 6(a). Therefore, the arrival angles are taken to be the average of these values. Taking array tilt into consideration, the arrival angles of B arrival impinging on the array are 47.4º, 18.8º and 13.4º, respectively (the corresponding source ranges are 5 km, 15.1 km and 24.2 km).

Secondly, spatial filters are designed to get the signals consisting of the B and SB arrivals based on the arrival angles of B arrival. It is noted that when the source and hydrophones are both near the ocean surface, the arrival angles of the B and SB arrivals are very close to each other. Consequently, the filtered signals contain both the two arrivals.

Finally, the time delay between the B and SB arrivals are estimated. Then based on Eq.(10) the ambiguity surfaces of the TDOA method are calculated and shown in Figure 6(b). The unit of the ambiguity surface is second. The results are ambiguous along curves which are contours of the time delays between the B and the SB arrivals as shown in Figure 1(c).

Combined method

It is noted that the real source locations are around the intersections of the straight striations in Figure 6(a) and the corresponding curves in Figure 6(b). The ambiguity surfaces using Eq.(11), which is the combination of the two ambiguity surfaces, are shown in Figure 6(c). The estimated locations are very close to the real source locations. In comparison, the results based on the MFP technique using the Bartlett processor are shown in Figure 6(d). The replica fields are calculated by the Bellhop model [11]. The localisation performance is poor due to the incompleteness of the bottom property and the array tilt.

SUMMARY

The modified WSF-MF technique is effective for source range estimation while the TDOA method has high resolution along the depth direction. The combination of the two methods shows much better performance than that of the MFP technique. It is because the replica fields include the phase and amplitude difference between all multipath arrivals. However, this information is influenced by the sound speed profile and the bottom properties greatly. In contrast, the arrival angles of some multipath arrivals and the time delays between the ocean-bottom-interface reflected arrivals (these arrivals do not penetrate into buried layers) are little affected by the uncertainty of the ocean environment. Therefore the presented method in this paper is robust.

ACKNOWLEDGMENTS

This work was supported by the National Natural Science Foundation of China (Grant No. 11174235) and the Doctorate Foundation of Northwestern Polytechnical University, China (Grant No. CX201226).

REFERENCES

[1] H. Schmidt, A. B. Baggeroer, W. A. Kuperman, and E. K. Scheer, "Environmentally tolerant beamforming for high-resolution matched field processing: Deterministic mismatch," *J. Acoust. Soc. Am.* **88**(4), 1851-1862 (1990).

[2] T. Zhang, K. Yang, and Y. Ma, "Matched-field localization using a virtual time-reversal processing method in shallow water," *Chinese Science Bulletin* **56**(8), 743-748 (2011).

[3] L. M. Zurk and B. H. Tracey, "Depth-shifting of shallow water guide source observations," *J. Acoust. Soc. Am.* **118**(4), 2224-2233 (2005).

[4] E. K. Skarsoulis and M. A. Kalogerakis, "Ray-theoretic localization of an impulsive source in a stratified ocean using two hydrophones," *J. Acoust. Soc. Am.* **118**(5), 2934-2943 (2005).

[5] R. Duan, K. Yang, Y. Ma, and B. Lei, "Research on reliable acoustic path: Physical properties and a source localization method," *Chin. Phys. B* **21**(12), 124301-124301 (2012).

[6] S. Pinson and L. Guillon, "Sound speed profile characterization by the image source method," *J. Acoust. Soc. Am.* **128**(4), 1685-1693 (2010).

[7] B. Ottersten, M. Viberg, P. Stoica, and A. Nehorai, "Exact and large sample maximum likelihood techniques for parameter estimation and detection in array processing," in *Radar Array Processing* ed: Springer, 1993, pp. 99-151.

[8] M. Viberg, B. Ottersten, and T. Kailath, "Detection and estimation in sensor arrays using weighted subspace fitting," *IEEE Trans. Signal Process.* **39**(11), 2436-2449 (1991).

[9] N. R. Chapman, "Measurement of the waveform parameters of shallow explosive charges," *The Journal of the Acoustical Society of America* **78**(2), 672-681 (1985).

[10] H. L. Van Trees, *Detection, estimation, and modulation theory*, John Wiley & Sons, New York, 2004.

[11] M. B. Porter and H. P. Bucker, "Gaussian beam tracing for computing ocean acoustic fields," *J. Acoust. Soc. Am.* **82**(4), 1348-1359 (1987).